



ELSEVIER

Contents lists available at ScienceDirect

Continental Shelf Research

journal homepage: www.elsevier.com/locate/csr

Research papers

Export of Pacific carbon through the Arctic Archipelago to the North Atlantic

E.H. Shadwick^{a,*}, H. Thomas^a, Y. Gratton^b, D. Leong^a, S.A. Moore^a, T. Papakyriakou^c, A.E.F. Prowe^d^a Department of Oceanography, Dalhousie University, Halifax, NS, Canada^b Institut National de Recherche Scientifique, Centre Eau, Terre et Environnement, Québec, QC, Canada^c Center for Earth Observation Science, University of Manitoba, Winnipeg, MB, Canada^d Leibniz-Institut für Meereswissenschaften, IFM-GEOMAR, D-24105 Kiel, Germany

ARTICLE INFO

Article history:

Received 11 March 2010

Received in revised form

20 January 2011

Accepted 31 January 2011

Available online 1 March 2011

Keywords:

Arctic Archipelago

Inorganic carbon system

International polar year (IPY)

ABSTRACT

During an east-to-west transect through the Canadian Arctic Archipelago, dissolved inorganic carbon (DIC) and total alkalinity (TA) were measured. The watermass composition throughout the Archipelago is determined using TA and the seawater oxygen isotope fractionation ($\delta^{18}\text{O}$) data, and the carbon characteristics of these waters are examined. The influence of the Mackenzie River is primarily limited to the upper water column in the western Archipelago while the fraction of sea-ice melt water in the surface waters increases eastward with maximum values at the outflows of Jones and Lancaster Sounds. The depth of Pacific-origin upper halocline waters increases eastward through the Archipelago. In the western Archipelago, non-conservative variations in deep water DIC are used to compute a subsurface carbon surplus, which appears to be fueled by organic matter produced in the surface layer and by benthic respiration. The eastward transport of carbon from the Pacific, via the Arctic Archipelago, to the North Atlantic is estimated, and the impact of increased export of sea-ice melt water to the North Atlantic is discussed.

© 2011 Elsevier Ltd. All rights reserved.

1. Introduction

In recent years much research has been devoted to understanding the ocean carbon cycle because of its prominent role in controlling global climate. Roughly half of the carbon dioxide (CO_2) released to the atmosphere from the burning of fossil fuels and other anthropogenic activities has been absorbed by the oceans (Sabine et al., 2004). Phytoplankton convert CO_2 to particulate organic carbon (POC), a portion of which is transported out of the surface layer by sinking, and therefore removed from the atmosphere. The oceans act as a significant reservoir for inorganic carbon, containing much more CO_2 than the atmosphere. Small changes in the ocean carbon cycle can therefore greatly influence atmospheric CO_2 concentrations (Zeebe and Wolf-Gladrow, 2001). Much attention has been given to the oceans' ability to take up anthropogenic carbon dioxide, and regions of deep water formation are of particular importance for this process. Seasonally ice-covered waters are sites of exceptionally high heat exchange, and may potentially transfer carbon dioxide into the deep ocean with greater efficiency than their lower latitude counterparts (Smith and Gordon, 1997; Miller et al., 2002). The Arctic Ocean and its carbon cycle in particular have been the subject of much recent study (e.g. Yager et al., 1995; Anderson et al.,

1998a,b; Fransson et al., 2001; Miller et al., 2002; Bates et al., 2005; Kaltin and Anderson, 2005; Mathis et al., 2005, 2007, 2009; Semiletov et al., 2007; Bates and Mathis, 2009; Chierici and Fransson, 2009; Yamamoto-Kawai et al., 2009; Mucci et al., 2010). The high-latitude oceans are ecologically sensitive areas where the impacts of climate changes may first be detected. Polar oceans are also chemically sensitive due to the relatively high Revelle factor and correspondingly weaker buffer capacity of these waters (Orr et al., 2005; Thomas et al., 2007; Chierici and Fransson, 2009; Fabry et al., 2009). The buffer capacity of seawater, described by the Revelle factor, determines its capacity to absorb CO_2 (Takahashi et al., 1993; Sabine et al., 2004). The Revelle factor quantifies the change in the seawater CO_2 partial pressure (pCO_2) for a given change in dissolved inorganic carbon (DIC), and is proportional to the ratio of DIC to total alkalinity (TA) (Revelle and Suess, 1957). Waters with low Revelle factors (e.g. 8–10) have a large potential capacity to absorb anthropogenic CO_2 and vice versa (Sabine et al., 2004). Warm tropical and subtropical waters have relatively low Revelle factor and therefore a large potential for the uptake of anthropogenic CO_2 , despite the lowered CO_2 solubility at high temperature. High latitude and polar oceans by contrast have relatively higher Revelle factors and a smaller potential capacity for the uptake of anthropogenic CO_2 (Sabine et al., 2004; Orr et al., 2005).

A greater understanding of the linkage between the export of freshwater from the Arctic Ocean to the North Atlantic and the dominant regional climate modes has emerged in recent years (Anderson et al., 2004; Peterson et al., 2006; Greene and Pershing, 2007). A positive North Atlantic Oscillation (NAO) enhances and

* Corresponding author. Now at: CSIRO and Antarctic Climate and Ecosystem Cooperative Research Center, Hobart, TAS, Australia.

E-mail address: elizabeth.shadwick@csiro.au (E.H. Shadwick).

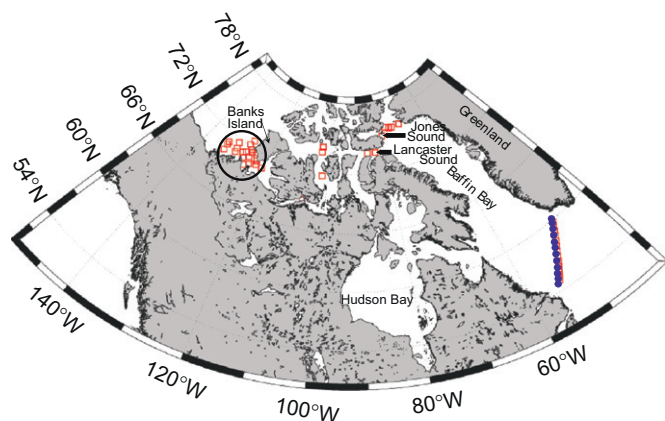


Fig. 1. Locations of stations sampled for dissolved inorganic carbon (DIC) and hydrographic data. Open squares indicate stations occupied in 2007, closed circles indicate stations from which an older data set from the Labrador Sea was used (Jones, 1998). The region indicated in the southwestern Archipelago by the circle is discussed in Section 5.1.

diverts the prevailing westerly winds, causing an eastward shift of the Eurasian river discharge and greater precipitation over Northern Europe (Thompson and Wallace, 2001). This eastward diversion of Eurasian runoff has been linked to a freshening of the Canada Basin (Macdonald et al., 2002). The Arctic Oscillation (AO) has also been linked to changes in circulation and associated distribution of freshwater in the Arctic Ocean (McLaughlin et al., 1996; Morison et al., 1998). Changes in freshwater export from the Arctic Ocean are thought to have consequences for North Atlantic Deep Water formation (Rahmstorf, 2002). It has been suggested that the decline in CO₂ uptake in the subpolar and temperate North Atlantic Ocean in the last decade is linked to the low or neutral NAO over the same period (Thomas et al., 2008). The export of DIC-rich Pacific-origin water from the Arctic Ocean may have implications for the uptake of atmospheric CO₂ in the North Atlantic, particularly in the northwestern region (Thomas et al., 2008). An understanding of the distribution and cycling of DIC in the waters of the Canadian Arctic Archipelago, which funnels roughly one third of the volume outflow from the Arctic Ocean (Coachman and Aagaard, 1974), is therefore of great importance to understanding carbon cycling in the Arctic Ocean as a whole.

We present DIC and TA measurements from west of Banks Island in the southeastern Beaufort Sea, eastward through the Archipelago to Jones and Lancaster Sounds (Fig. 1). These data were collected on an ArcticNet cruise on board the Canadian Coast Guard Ship *Amundsen*. Inorganic carbon data were complemented by measurements of the seawater oxygen isotope ratio ($\delta^{18}\text{O}$) and hydrographic variables. The relative contributions of (1) meteoric water, (2) sea-ice melt (3) Pacific-origin upper halocline water, and (4,5) two sources of Atlantic water: from the Arctic interior, and from Baffin Bay via Nares Strait and the West Greenland current were computed. The corresponding eastward transport of carbon through the Archipelago to Baffin Bay is estimated. The impact of an increasing fraction of sea-ice melt in the waters exported from the Archipelago on the pH and aragonite saturation state in downstream waters is discussed. Non-conservative variations in deep-water DIC at stations located in the southwestern Archipelago are used to compute a carbon surplus, or respiratory carbon inventory, in this region.

2. Oceanographic setting

The Arctic Ocean is the most land dominated of the ocean basins, almost entirely enclosed by the wide Siberian Shelf and

the numerous islands of the Canadian Arctic Archipelago. Atlantic waters enter the Arctic Ocean through Fram Strait and the Barents Sea. These waters flow cyclonically around the Arctic Basin, exiting via Fram Strait, Nares Strait, and the many channels of the Canadian Arctic Archipelago (Rudels et al., 1994, 1996). Pacific water enters the Arctic Ocean through the relatively narrow and shallow Bering Strait (Coachman and Aagaard, 1988). In the Beaufort Sea, circulation is dominated by the Beaufort Gyre, a wind-driven circulation caused by a mean anticyclonic high pressure dome in the atmosphere (Carmack and MacDonald, 2002). This feature maintains the high concentrations of sea-ice in the central Arctic Ocean (Macdonald et al., 1999). The surface circulation in the Beaufort Sea is dominated by the anticyclonic Beaufort Gyre. The flow of subsurface waters is reversed, dominated by the cyclonic Beaufort Undercurrent (Carmack and MacDonald, 2002). This undercurrent forces waters of both Pacific and Atlantic origin to the east along the continental margin, providing (offshore) nutrients to the Arctic shelves (Macdonald et al., 1987; McLaughlin et al., 2004).

In winter, the Arctic Ocean is sea-ice covered, except in polynyas and flaw leads, with multi-year ice in the central Arctic Ocean and thinner seasonal ice-cover on the shelves. The seasonal production and melting of sea-ice makes a significant contribution to the mixing of water masses in the Arctic Ocean (Carmack and Chapman, 2003). Sea-ice melt and brine rejection during sea-ice formation modify the physical and chemical properties of the surface and halocline layers (Steele and Boyd, 1998; Carmack and Chapman, 2003).

The Arctic Ocean and adjacent polar continental seas play an important role in the biogeochemical cycling of carbon and nutrients. There are large reservoirs of terrestrial and oceanic carbon in the Arctic region (Dittmar and Kattner, 2003; Hansell et al., 2004; Mathis et al., 2007), and many uncertainties in the response of these stocks to projected climate shifts. The Arctic shelf seas host high rates of primary production during the brief photosynthetic season (Carmack et al., 2004; Arrigo et al., 2008; Mathis et al., 2009). Sea-ice cover controls the availability of light, and limits the development of water column stratification. Despite available nutrients in spring, the light environment may inhibit the growth of phytoplankton until surface stratification, due to solar heating, or sea-ice melt, is achieved in summer (Arrigo et al., 2008; Tremblay et al., 2008). The Arctic Ocean continental shelves have been classified as 'inflow', 'interior' and 'outflow' (Carmack and Wassmann, 2006). The Barents and Chukchi Seas can be characterized as inflow shelves, importing nutrient-rich (and carbon-rich) water from the Pacific and Atlantic Oceans to sustain the relatively high seasonal production in these regions (Cota et al., 1996; Carmack and Wassmann, 2006; Bates et al., 2009). The East Siberian and Beaufort Sea shelves are characterized as interior shelves which are under the influence of other adjacent shelf environments. The Canadian Arctic Archipelago constitutes an outflow shelf through which water from the Arctic Ocean is exported to the North Atlantic via Baffin Bay.

There have been relatively few studies of the Canadian Arctic Archipelago with respect to the carbonate system (Bates and Mathis, 2009; Macdonald et al., 2009; Shadwick et al., 2011). In this region, as in other Arctic shelf regions, the inorganic carbon cycle is influenced by both physical and biological processes (Anderson et al., 1998a; Bates et al., 2005; Bates and Mathis, 2009; Shadwick et al., 2011). Air–sea exchange of CO₂ and other gasses takes place primarily during seasonal sea-ice retreat, and also during the winter months in leads and polynyas, which may have a significant impact on water column ventilation (Falkner et al., 2005). Vertical and horizontal mixing of water masses and the addition of freshwater from runoff and sea-ice melt play an important role (Carmack et al., 2004; Chierici and Fransson,

2009). In the open water season, inorganic carbon is taken up by phytoplankton and organic matter subsequently exported from the surface to the subsurface (Bates et al., 2005; Mathis et al., 2007; Shadwick et al., 2011). These processes will be explored in more detail in Section 4.1.

3. Data and methods

3.1. Sample collection and analysis

Samples were collected at 31 stations throughout the Canadian Archipelago from Baffin Bay westward to Banks Island (Fig. 1) during September and October, 2007. Approximately 500 samples were collected from the surface to depths of roughly 600 m, with higher vertical resolution within the euphotic zone (0–50 m), at all stations (Fig. 1). Dissolved inorganic carbon (DIC) and total alkalinity (TA) samples were collected from 10-L Niskin bottles mounted on a General Oceanic 24-bottle rosette fitted with a SeaBird CTD such that all chemical data are associated with high precision in situ temperature, salinity and oxygen data. Following water collection, DIC and TA samples were poisoned with a solution of HgCl_2 to halt biological activity and stored in the dark at 4 °C to await analysis. All DIC and TA samples were analyzed on board by coulometric, and potentiometric titration, respectively, using a VINDTA 3C (versatile instrument for the determination of titration alkalinity, by Marianda). Analytical methods for determination of DIC and TA have been fully described elsewhere (Johnson et al., 1993; Fransson et al., 2001; Bates et al., 2005). Routine analyses of Certified Reference Materials (provided by A. G. Dickson, Scripps Institution of Oceanography) ensured that the uncertainty of the DIC and TA measurements was less than 1 and 2 $\mu\text{mol kg}^{-1}$, respectively. Following the determination of DIC and TA, we computed pH (on the total scale, with an estimated uncertainty of 0.05) and aragonite saturation (Ω_{Ar} , with an estimated uncertainty of 0.1) using the standard set of carbonate system equations, excluding nutrients, with the CO_2Sys program of Lewis and Wallace (1998). We used the equilibrium constants of Mehrbach et al. (1973) refit by Dickson and Millero (1987). The calcium (Ca^{2+}) concentration was assumed to be conservative and calculated from salinity. For a complete description of the carbonate system in seawater see, for example, Zeebe and Wolf-Gladrow (2001), and for the Arctic in particular, Bates and Mathis (2009) or Chierici and Fransson (2009).

3.2. Water mass definitions

Previous studies have reported various classifications and names for the portions of the Arctic Ocean water column (Anderson et al., 1994; Jones et al., 1998; Ekwurzel et al., 2001). The water masses of the Arctic ocean can be simplistically classified based on their salinities (Aagaard et al., 1981; Aagaard and Carmack, 1994; Mathis et al., 2005). The polar mixed layer (PML) is defined by salinity $29.5 < S < 31$ (following the range of salinity values for the Canada Basin reported by Yamamoto-Kawai and Tanaka, 2005). The PML is a mixture of meteoric water (MW), sea-ice melt (SIM) and Pacific-origin upper halocline water. A fourth water mass of Atlantic origin (ATL, $S > 34.8$) is also present.

In general, knowing the $\delta^{18}\text{O}$ and TA of all water masses in a three end-member system and assuming conservative behavior, one can compute their relative fractions in a seawater sample with known $\delta^{18}\text{O}$ and TA (e.g. Fransson et al., 2001; Anderson et al., 2004; Yamamoto-Kawai and Tanaka, 2005). It was assumed that the upper 150 m of the water column comprised MW, SIM

and UHL and the following system of equations was used:

$$f_{\text{MW}} + f_{\text{SIM}} + f_{\text{UHL}} = 1 \quad (1)$$

$$\delta^{18}\text{O}_{\text{MW}}f_{\text{MW}} + \delta^{18}\text{O}_{\text{SIM}}f_{\text{SIM}} + \delta^{18}\text{O}_{\text{UHL}}f_{\text{UHL}} = \delta^{18}\text{O} \quad (2)$$

$$\text{TA}_{\text{MW}}f_{\text{MW}} + \text{TA}_{\text{SIM}}f_{\text{SIM}} + \text{TA}_{\text{UHL}}f_{\text{UHL}} = \text{TA} \quad (3)$$

For depths greater than 150 m, it was assumed that the water column comprised UHL, ATL and net SIM, and the following system of equations was used:

$$f_{\text{SIM}} + f_{\text{UHL}} + f_{\text{ATL}} = 1 \quad (4)$$

$$\delta^{18}\text{O}_{\text{SIM}}f_{\text{SIM}} + \delta^{18}\text{O}_{\text{UHL}}f_{\text{UHL}} + \delta^{18}\text{O}_{\text{ATL}}f_{\text{ATL}} = \delta^{18}\text{O} \quad (5)$$

$$\text{TA}_{\text{SIM}}f_{\text{SIM}} + \text{TA}_{\text{UHL}}f_{\text{UHL}} + \text{TA}_{\text{ATL}}f_{\text{ATL}} = \text{TA} \quad (6)$$

The end-member values used in the analysis are given in Table 1. The TA associated with the MW fraction is the flow-weighted average of the Mackenzie River (Cooper et al., 2008). Additional North American rivers flow into the Beaufort Sea and Canadian Arctic Archipelago and these freshwater sources likely have somewhat different TA (and DIC) than the Mackenzie River (Shadwick et al., 2011), which adds to the uncertainty of the estimate of the MW fraction computed here. The $\delta^{18}\text{O}$ value associated with the MW fraction of Khatiwala et al. (1999) for Arctic rivers was used. Direct precipitation minus evaporation over land is accounted for in the MW end-member, and will have the same properties as the runoff. Precipitation minus evaporation occurring over the ocean adds freshwater ($S=0$) with $\text{TA}=0$. This contribution comprises only a small input of the total freshwater flux to the Arctic region (Serreze et al., 2006) and this contribution has been neglected by assigning the Mackenzie River value to the TA end-member for MW. We have assumed that the salinity and TA of SIM are null, i.e., sea-ice does not constitute a net source of salinity or TA to the underlying seawater. The salinity and TA trapped in the sea-ice during formation are subsequently released during ice melt. The end-member TA and $\delta^{18}\text{O}$ associated with the UHL fraction were determined from the mean values corresponding to a salinity of 33.1 at all stations. The end-member TA and $\delta^{18}\text{O}$ associated with the ATL were the mean values corresponding to the temperature maximum at each station following Yamamoto-Kawai and Tanaka (2005).

The error associated with the MW and SIM fraction was estimated between 1% and 3% (Yamamoto-Kawai and Tanaka, 2005). The error associated with the UHL and ATL were somewhat higher between 10% and 14% (Jones et al., 1998; Yamamoto-Kawai and Tanaka, 2005). The water mass computations described above were made using $\delta^{18}\text{O}$ and TA as conservative tracers. The analysis was repeated using $\delta^{18}\text{O}$ and salinity and the results were not different from those presented in the following sections. While there is more natural variability in TA than salinity, since the focus of this work is the inorganic carbon system, we elected to present the results obtained using $\delta^{18}\text{O}$ and TA despite the potential for larger error in the water mass fractions.

Table 1
End-member properties used in the three component mass balance equations.

Water mass	Salinity	$\delta^{18}\text{O}$ (‰)	TA ($\mu\text{mol kg}^{-1}$)	DIC ($\mu\text{mol kg}^{-1}$)
MW	0	−20	1540	1390
SIM	0	−2.0	0	0
UHL	33.1	−1.5	2283	2236
ATL	34.8	0.19	2301	2154

4. Results

4.1. Water mass composition

The fractions of MW and SIM in three regions are shown in Fig. 2. These profiles are computed from average values of (a) five stations located west of Banks Island, in the southeastern Beaufort Sea; (b) three stations centrally located in the Canadian Archipelago; and (c) three stations within the outflow of Lancaster Sound to Baffin Bay (see also Fig. 1). In the western region (Fig. 2a), MW amounted to roughly 3% in the upper 40 m of the water column. Over the same depth range SIM was roughly 5%. Below 60 m, MW was between 0% and 1% while SIM in this depth range amounted to between 0% and 2%. In the central region (Fig. 2b), the fraction of MW in the upper 20 m was roughly 1%, with a peak value of roughly 3% at 30 m and values of MW < 1% below 40 m. In the same region, the SIM fraction was roughly 6% in the upper 20 m and ranged from 1% to 2% below a depth of 40 m. At the eastern stations in Lancaster Sound (Fig. 2c), the MW fraction ranged from 0% to less than 1%. In the same region, the SIM fraction reached the maximum value of nearly 8% in the upper 20 m of the water column. Below a depth of 40 m in Lancaster Sound, the SIM fraction ranged from roughly 2% to 3%. The depth of penetration of the PML increases eastward through the Archipelago, while the fraction of SIM water increases. This may be due to increased sea-ice formation and brine rejection.

In the western region the fraction of UHL ranged from 93% at the surface to 100% at a depth of 130 m; below 200 m the fraction of ATL was 100% (see Table 2). In the central region, the fraction of UHL ranged from 94% at the surface to 100% at a depth of 120 m; at a depth of 140 m the fraction of UHL was 95% and ATL was 5%. In the eastern region in Lancaster Sound at a depth of 130 m the fraction of SIM was 1% and UHL was 98%. At a depth of 400 m the SIM fraction was 1%, UHL was 51% and ATL was 48%. At a depth of 500 m in Lancaster Sound the SIM fraction was 0%, UHL was 51% and ATL was 49%, indicating that the depth of penetration of UHL increases through the Archipelago in the eastward direction, towards Baffin Bay (see Table 2). The penetration of Pacific water to greater depths in the central and eastward stations (relative to the westward stations) results from shallow sill depths in the Arctic Archipelago, limiting the penetration of Atlantic waters (Münchow et al., 2007). The ATL water present in the deep

samples from the Lancaster Sound region is Atlantic water coming both from the south via the West Greenland Current (WGC), and from the north via Nares Strait, and not Atlantic water from the Beaufort Sea region of the Arctic. Previous studies have reported a mixing of UHL and Atlantic-derived WGC waters in the North Water region of Baffin Bay (Münchow et al., 2007; Melling et al., 2001; Miller et al., 2002; Lobb et al., 2003).

4.2. The carbonate system

The distributions of DIC, TA, pH, and Ω_{Ar} with depth for the three regions described in the preceding section are shown in Figs. 3 and 4. DIC profiles reflect the influence of freshwater and biology at the surface, both of which decrease DIC concentrations. The lowest surface DIC concentrations ($\sim 1925 \mu\text{mol kg}^{-1}$) are observed in the western region, where the combined input of MW and SIM amounts to roughly 7% of the water in the upper 40 m. In the eastern region, where the dilution of the surface waters is primarily due to SIM (roughly 8%) which does not contribute DIC (see Table 1), the minimum surface DIC concentration ($\sim 1970 \mu\text{mol kg}^{-1}$) is enhanced relative to the western station. This may indicate a larger contribution from surface primary production in the western region, which would decrease surface DIC concentrations. The surface waters in the western region are most influenced by MW, primarily from the nearby Mackenzie River. The Mackenzie River is supersaturated with the

Table 2

Water mass composition in three regions: western—west of Banks Island, central—centrally located in the Archipelago, and eastern—near the outflow of Lancaster Sound (Fig. 1). The values are listed as percentages.

Region	Depth	SIM	UHL	ATL
Western	130	0	100	0
	≥ 200	0	0	100
Central	120	0	100	0
	140	0	95	5
Eastern	130	1	98	1
	400	1	51	48
	500	1	51	49

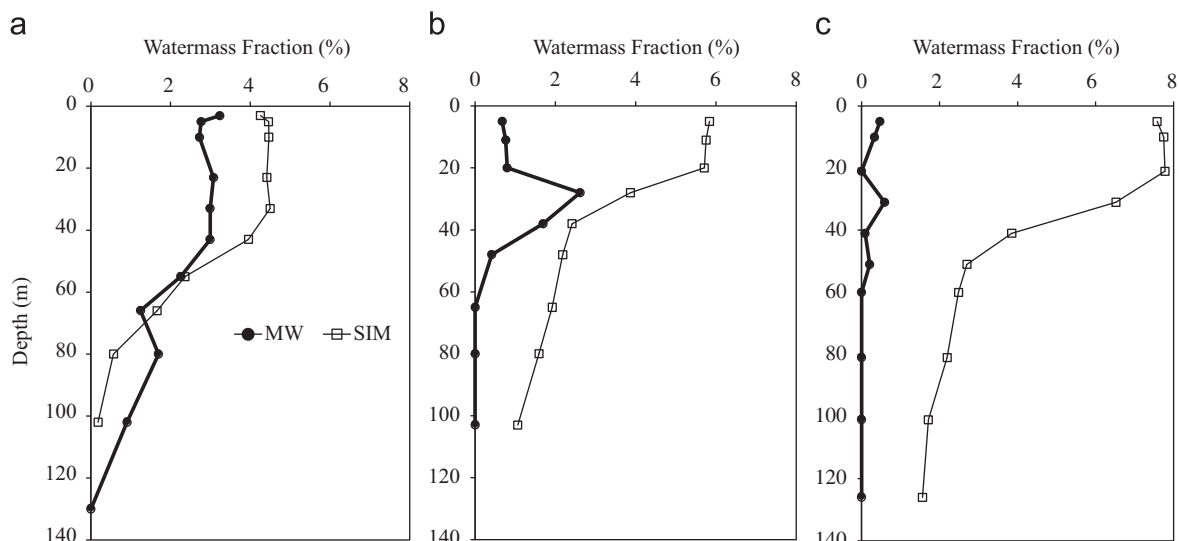


Fig. 2. Fractions of MW and SIM for an average of stations located in (a) west of Banks Island, (b) centrally located in the Canadian Archipelago, and (c) located near the outflow of Lancaster Sound to Baffin Bay. Please note that only the upper water column is shown.

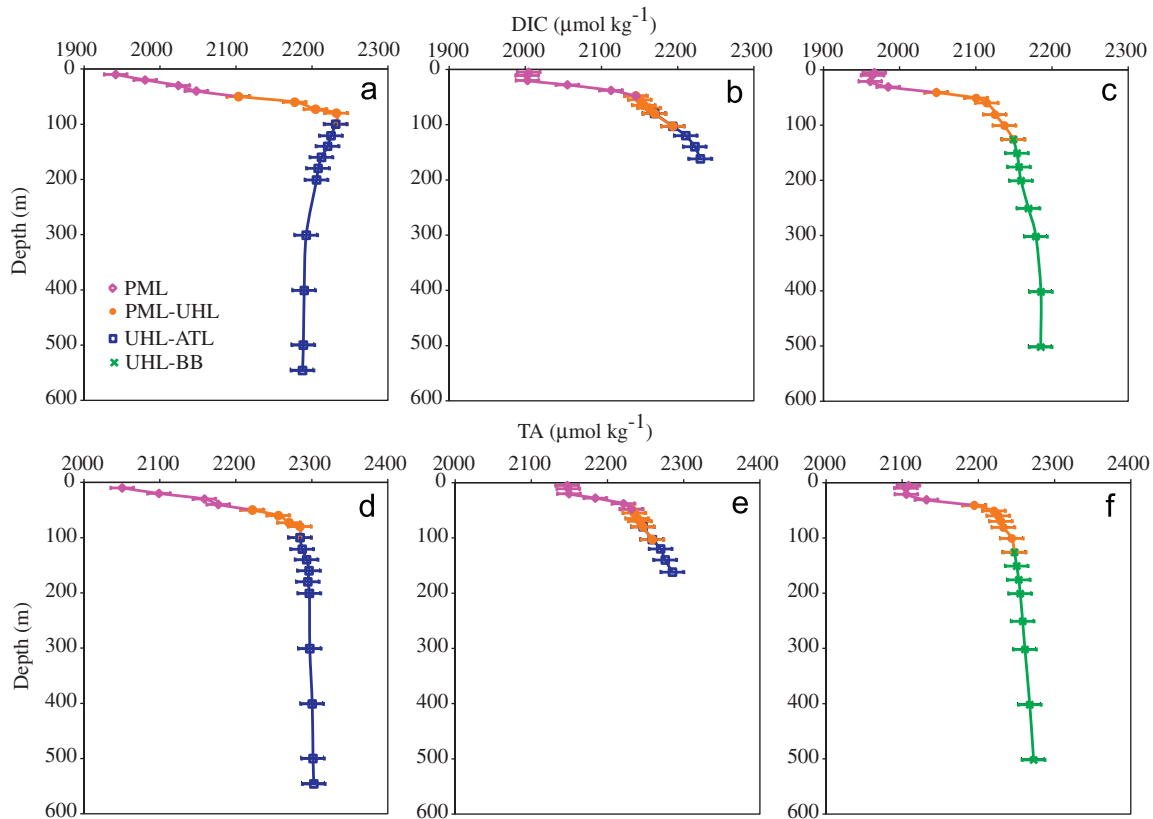


Fig. 3. Profiles of DIC and TA for an average of stations located (a,d) west of Banks Island, (b,e) centrally located in the Canadian Archipelago, and (c,f) located near the outflow of Lancaster Sound to Baffin Bay, with the dominant water masses identified. The PML comprised MW, SIM, and UHL water. The error bars are the standard deviation associated with the mean DIC and TA values. The range in values reflects spatial variability rather than measurement uncertainty.

respect to the atmosphere with $p\text{CO}_2$ of the order of $700 \mu\text{atm}$ (Vallières et al., 2008) and correspondingly low pH.

The influence of runoff from the Mackenzie River is seen in the low surface pH values in the western region relative to the central and eastern regions where the effect of MW is diminished (Figs. 2 and 4). The aragonite saturation state (Ω_{Ar}) decreases with increasing SIM due to the dilution of chemical constituents with the addition of freshwater (Bates and Mathis, 2009; Chierici and Fransson, 2009). This reduction is seen in the upper 30 m of the water column in the central and eastern regions corresponding to the largest values of SIM fraction (Figs. 2 and 4). However, the lowest surface values of Ω_{Ar} were observed at the western station where the smallest contribution from SIM was computed (Figs. 2a and 4a). The DIC minimum observed in the western region is likely the result of biological production during the preceding growing season which increases the surface Ω_{Ar} . However, the western region is under the additional influence of Mackenzie River runoff. The input of MW and SIM to the surface waters in this region outweighs the biologically mediated increase in Ω_{Ar} and results in the low observed surface values (see also Shadwick et al., 2011).

There is a subsurface DIC maximum at a depth of roughly 100 m in both the western ($\sim 2230 \mu\text{mol kg}^{-1}$) and eastern ($\sim 2150 \mu\text{mol kg}^{-1}$) regions, although this feature is less pronounced in the eastern region. This subsurface increase in DIC is due to the large fraction of (carbon-rich) UHL water at this depth, and also indicates the remineralization of organic matter. Below a depth of roughly 120 m in the western region there is a modest decrease in DIC with depth indicating the influence of relatively lower-DIC ATL waters in this region of the water column. The DIC concentrations are notably higher at the depth range of 100–200 m in the central region than is seen at the same depth

in the western region, while TA in the central region is reduced relative to the western region. The pH over this same depth range decreases in the central region, while there is an increase in pH in the western region. We propose that organic matter remineralization over the shallow sill at the central location, which increases DIC relative to TA, is the reason for the observed elevated DIC, and reduced pH in this region. The bottom waters (below 200 m) in the western region have higher concentration of TA than the waters at the same depth in the eastern region. This is due to the composition of the deep water, which in the western region has a larger fraction of ATL, with lower DIC and higher TA (and salinity), while in the eastern region, at the outflow of Lancaster Sound, the contribution of ATL at this depth is reduced, lowering the TA (and salinity) relative to the western region.

The range of DIC and TA concentration over all measured samples throughout the Archipelago is quite broad (Fig. 5). The relationships between DIC and salinity and TA and salinity are shown in Fig. 5a and b. The lowest concentrations of DIC ($< 1800 \mu\text{mol kg}^{-1}$) and TA ($\sim 1850 \mu\text{mol kg}^{-1}$) are associated with the salinity minimum ($S \sim 26$) resulting from contributions from both MW and SIM to the PML. The extrapolation to $S=0$ of a linear regression of DIC (and TA) for all samples with $\text{MW} > 0$ and/or $\text{SIM} > 0$ in the upper 50 m of the water column yields values for the MW end-member of: $\text{DIC} = 1390 \mu\text{mol kg}^{-1}$ and $\text{TA} = 1425 \mu\text{mol kg}^{-1}$, roughly consistent with the flow-weighted Mackenzie River value of TA used in the MW fraction computation of Cooper et al. (2008) (see Section 3.2 and Table 1).

From the surface to a depth of roughly 150 m, covering the salinity range from 26 to roughly 31, DIC concentration ranged from less than $1800 \mu\text{mol kg}^{-1}$ to greater than $2250 \mu\text{mol kg}^{-1}$. The TA concentration increased from roughly 1850 to $2250 \mu\text{mol kg}^{-1}$ over the same range of depth (0–150 m) and salinity (from $S=26$ to ~ 31). The DIC

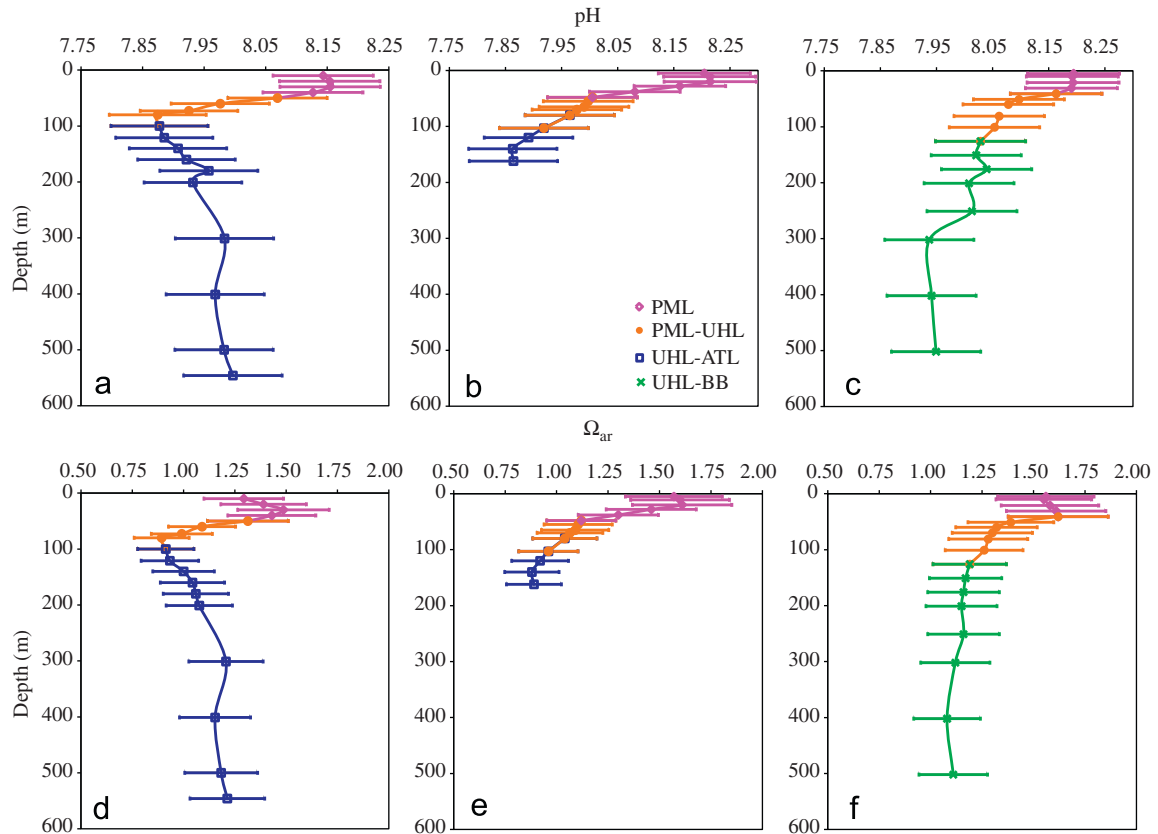


Fig. 4. Profiles of pH and Ω_{Ar} for an average of stations located (a,d) west of Banks Island, (b,e) centrally located in the Canadian Archipelago, and (c,f) located near the outflow of Lancaster Sound to Baffin Bay with the dominant water masses identified. The PML comprised MW, SIM, and UHL water. The error bars are the standard deviation associated with the mean pH and Ω_{Ar} values. The range in values reflects spatial variability rather than measurement uncertainty.

maximum (of the order of $2240 \mu\text{mol kg}^{-1}$) is coincident with the maximum fraction of UHL (at $S=33.1$). The TA maximum (of the order of $2300 \mu\text{mol kg}^{-1}$) is coincident with the maximum fraction of ATL and the salinity maximum ($S=34.88$). The ratio between DIC and TA is roughly 1:1 in the PML (Fig. 5c). This ratio increases slightly to 1.2:1 in the UHL as a result of the remineralization of organic matter which increases DIC relative to TA. In the deeper water column, and for salinities $S > 33$, ATL water dominates and the concentration of TA continues to increase (relative to the PML and UHL) primarily as a function of increasing salinity. The concentration of DIC in the ATL water is reduced, relative to the UHL due to the reduction of respiration, or remineralization of organic matter, as a function of depth. The pH of the surface waters ranges from roughly 8.05 to 8.15 (Fig. 5d). The pH maximum, roughly 8.20, occurs in the PML and is associated with salinities of roughly 31. The eastward increase in the depth of penetration of PML water may have consequences for the uptake of atmospheric CO_2 . A deeper PML, with relatively lower DIC and relatively higher pH (Fig. 5a and d) may lead to enhanced CO_2 uptake eastward through the Archipelago. The pH minimum, of the order of 7.80, is associated with the maximum fraction of UHL and reflects the high concentrations of DIC in the Pacific-origin waters.

While there has been some debate as to the utility of the salinity normalization in the analysis of water mass properties, particularly in the coastal zone (Friis et al., 2003; Robbins, 2001), we find that salinity-normalized DIC, (DIC_{norm}), though not a conservative tracer, is a powerful parameter in the identification of water masses and mixing relationships. In brief, the normalization of DIC to a constant salinity removes the effect of freshwater fluxes from the measured DIC concentrations. DIC_{norm} is thus primarily controlled by the water temperature (i.e., by the solubility of CO_2), biological processes, air–sea exchange of CO_2 ,

and by the mixing of water masses. Furthermore, the use of DIC_{norm} allows us to determine whether non-conservative processes, such as biological production or air–sea CO_2 flux, are dominant at the timescales over which mixing occurs. DIC was normalized to a regional mean salinity of $S^{\text{mean}}=32.5$, computed using all samples collected at all stations indicated in (Fig. 1), (i.e. $\text{DIC}_{\text{norm}}=32.5 \text{ DIC}/S$). Because the application of a salinity normalization as described above is not appropriate for waters subject to riverine influence, due to the non-zero concentration of DIC in the river water, samples with a MW component were normalized following (Friis et al., 2003):

$$\text{DIC}_{\text{norm}} = \frac{(\text{DIC}^{\text{obs}} - \text{DIC}^{S=0})}{S^{\text{obs}}} S^{\text{mean}} + \text{DIC}^{S=0} \quad (7)$$

where the superscript 'obs' refers to the observed value.

The relationship between DIC_{norm} and salinity is shown in Fig. 6, and four mixing regimes are identified. In the low-salinity surface waters the mixing of MW, SIM and UHL waters form the PML. As previously discussed the contribution from MW decreases with distance from the Mackenzie river, with MW fractions at the easternmost stations of less than 1%. The salinity-normalized DIC allows most MW with high DIC_{norm} to be distinguished from sea-ice melt, represented by the y-intercept of the orange line in Fig. 6, with a much lower DIC concentration (see Table 1). Mixing can be clearly identified as the dominant process between the PML and UHL water, observed at most stations throughout the Archipelago in the depth range of roughly 30–100 m. Over the given time scale, mixing dominates while the effects of non-conservative processes can hardly be determined, if at all, from the corresponding data. Mixing of ATL and UHL was found in the deepest waters. Samples from the western region

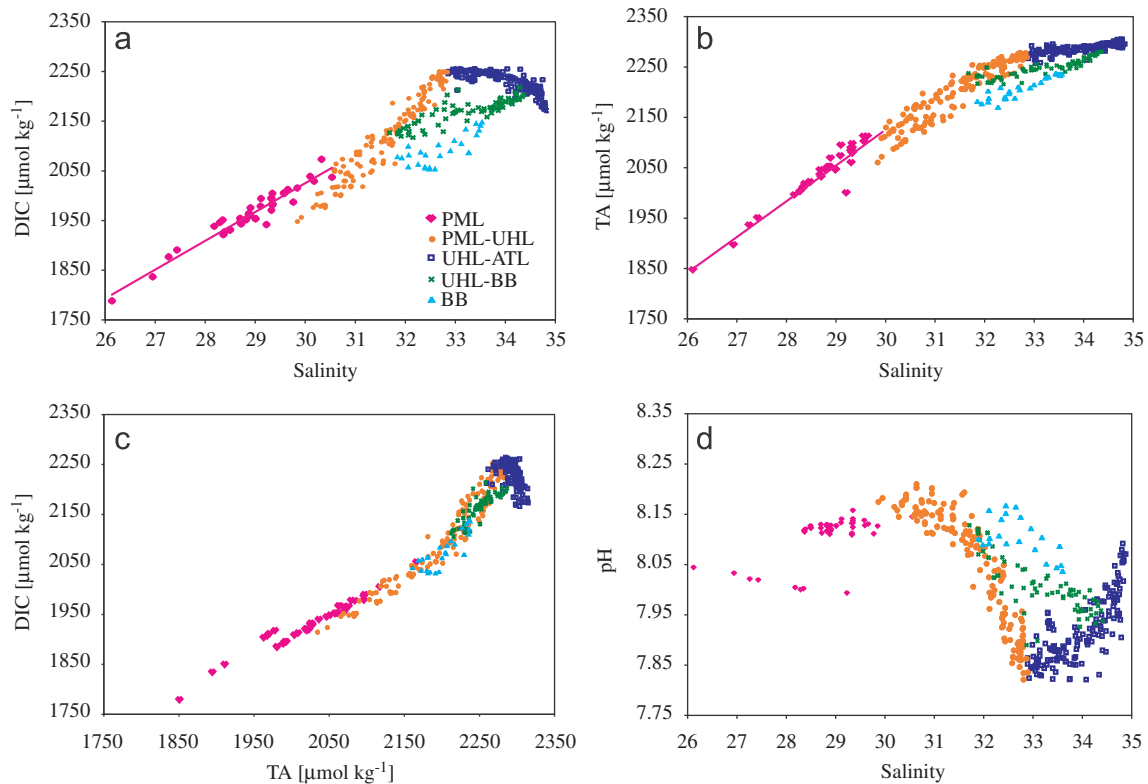


Fig. 5. (a) Dissolved inorganic carbon (DIC) versus salinity, (b) TA versus salinity, (c) DIC versus TA and (d) pH versus salinity for samples collected at the stations indicated by the red squares in Fig. 1. Five water masses are identified: PML (pink diamonds), PML-UHL (orange dots), UHL-ATL (blue squares), and UHL-BB (green x's). Surface water samples from stations located in the North Water region of Baffin Bay are plotted in pale blue. These waters result from a contribution from sea-ice melt which adds water with $S=0$, with very low DIC concentration. The color coding is according to the water mass identification revealed in Fig. 6. The solid lines in panels (a) and (b) indicate linear regressions of the surface samples to determine the DIC and TA at $S=0$.

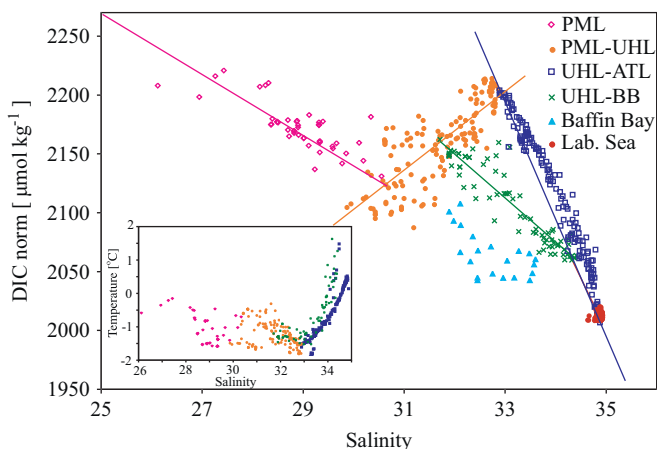


Fig. 6. Salinity normalized DIC versus salinity. Five idealized mixing lines are indicated: PML (pink diamonds), PML-UHL (orange dots), UHL-ATL (blue squares), and UHL-BB (green x's) and WGC-Labrador Sea (red). Surface water samples from stations located in the North Water region of Baffin Bay are plotted in pale blue. These waters result from a contribution from sea-ice melt, which adds fresh water, while making a negligible addition of DIC, in contrast to the fresh water addition from rivers which has a much higher DIC concentration. Inset: a $T-S$ plot with the same color coding as in the DIC_{norm} versus salinity plot. The two Atlantic-origin water masses (in blue and green) are clearly distinguishable, while the PML and UHL have a wider range of both temperature and salinity.

(Fig. 6, in blue; i.e. west of $100^{\circ}W$), display the least amount of scatter about the proposed idealized 'mixing line'. The non-conservative behavior seen in the UHL and ATL samples collected in the western region is, as discussed in Section 5.1, due to the

remineralization of organic matter. The fourth mixing regime is between UHL and Baffin Bay ATL source water of slightly lower salinity and higher DIC relative to samples from the western region (Fig. 6, in green). The contribution of ATL water seen at stations in Jones and Lancaster Sounds does not originate from the Archipelago, but from Baffin Bay or Nares Strait. This is consistent with Jones et al. (2003), who, using nutrient ratios as water mass tracers, found no Atlantic water, from the Arctic interior, in the outflow from either Lancaster or Jones Sound.

5. Discussion

5.1. Deep water carbon storage

The mixing of Pacific and Atlantic waters in the lower water column of the westernmost stations, clustered in the southeastern Beaufort Sea region, southwest of Banks Island (see circled region in Fig. 1) is now investigated in more detail. If DIC concentrations observed in the range of mixing of UHL and ATL waters resulted only from conservative mixing, all samples should fall along the proposed 'mixing line' (shown in blue in Fig. 6). The bowed structure of the relationships between DIC and salinity (Fig. 5a, in blue) and DIC_{norm} and salinity (Fig. 6) and the deviation from the general linear trend in the plot of DIC versus TA (Fig. 5c, in blue), imply that another, non-conservative process is at play. This process is assumed to be the result of biological activity, and not air-sea exchange, due to the depth range of the waters (from roughly 80 to 600 m). Further confirmation that this is indeed a biological process is the absence of

a water mass with high salinity ($S \geq 34$), and high DIC ($\text{DIC} > 2250 \mu\text{mol kg}^{-1}$), that would act as a third end member, attributing this bowed structure to a physical process. Non-conservative variations in DIC are thus attributed to biology ($\Delta\text{DIC}_{\text{bio}}$), and can be expressed as the differences between the expected (DIC_{ex}) (i.e. the idealized mixing) and the observed (DIC_{obs}) values:

$$\Delta\text{DIC}_{\text{bio}} = \text{DIC}_{\text{obs}} - \text{DIC}_{\text{ex}} \quad (8)$$

Negative values of $\Delta\text{DIC}_{\text{bio}}$ correspond to inorganic carbon deficits implying that production exceeds respiration in the system. Conversely, positive values of $\Delta\text{DIC}_{\text{bio}}$ imply that respiration exceeds production and correspond to a surplus of inorganic carbon. Profiles of DIC_{ex} are computed from salinity and the following relationship: $\text{DIC}_{\text{ex}} = -48.24S + 3832$ derived from the DIC and salinity of the UHL and ATL end-members (see Table 1) and shown graphically by the idealized mixing line in Fig. 7a. Using Eq. (8), $\Delta\text{DIC}_{\text{bio}}$ was computed for each sample. These values were integrated over the depth range of UHL and ATL waters, as prescribed by their salinities, and a mean value of $\text{DIC}_{\text{bio}} = 5.8 \pm 0.2 \text{ mol C m}^{-2}$, subsequently referred to as ‘carbon surplus’, was computed. Further confirmation that biology is driving the increased DIC concentrations is evident from a plot of apparent oxygen utilization (AOU) for the same discrete samples (Fig. 7). A bowed structure analogous to that of DIC is also found in the AOU distribution. As in the case of DIC, AOU is integrated over the same range of salinity, and we find a total oxygen utilization of $7.7 \pm 0.5 \text{ mol O}_2 \text{ m}^{-2}$, yielding a ratio of

$\text{AOU}:\text{DIC} = 1.22$, consistent with the Redfield ratio of $\text{O}_2 : \text{CO}_2 = 138 : 106 \approx 1.30$ (Millero, 2006).

The remineralization of organic carbon in the subsurface waters, derived from primary production in the euphotic zone, results in the excess carbon seen in the deep water. Assuming that the residence time for subsurface water in the southeastern Beaufort Sea is of the order of 1–2 years (Lanos, 2009), we arrive at a carbon draw down ranges from 2.9 to 5.8 $\text{mol C m}^{-2} \text{ yr}^{-1}$ (with a mean value of 4.4 $\text{mol C m}^{-2} \text{ yr}^{-1}$). This estimate is in general agreement with the rather sparse primary production data for this region, which ranges from 7 to 15 $\text{mol C m}^{-2} \text{ yr}^{-1}$ (Arrigo and van Dijken, 2004). This calculated respiratory carbon surplus corresponds to an export production of roughly 30–60% of the primary production. A recent estimate of vertical export in the region suggests that roughly 2 $\text{mol C m}^{-2} \text{ yr}^{-1}$, or less than 20% of primary production, leaves the surface layer (Jull-Pedersen et al., 2010). Sediment trap data from the southeastern Beaufort Sea indicates that roughly 0.45 $\text{mol C m}^{-2} \text{ yr}^{-1}$ of marine particulate organic carbon (POC) reaches a depth below 200 m, with an additional contribution from terrestrial sources (Forest et al., 2008) which implies a subsurface respiration of only 1.55 $\text{mol C m}^{-2} \text{ yr}^{-1}$. An additional source of inorganic carbon to the subsurface layer is benthic respiration which may be significant in this region (Renaud et al., 2007; Shadwick et al., 2011). Alternatively a portion of the subsurface respiration estimated here may be fueled by organic material delivered laterally to the region from the adjacent Mackenzie Shelf waters which contain a significant pool of POC (Macdonald et al., 1987).

5.2. Carbon export to the North Atlantic

The Beaufort Sea communicates with the Atlantic Ocean through Fram Strait, and those passages in the Arctic Archipelago that enter Baffin Bay. Lancaster Sound, Nares Strait and Jones Sound all exit the Archipelago to Baffin Bay. Several estimates of volume transport from the Archipelago from Jones and Lancaster Sound have been made (Rudels, 1986; Cuny et al., 2005; Prinsenberg and Hamilton, 2005). We applied the estimate of Ingram et al. (2002), which assumes that the net eastward outflows from Jones Sound and Lancaster Sounds are 0.3×10^6 and $1.1 \times 10^6 \text{ m}^{-3} \text{ s}^{-1}$, respectively. Multiplying this volume transport by the water column DIC inventories in Jones and Lancaster Sounds yields an estimate of carbon exported from the Archipelago to Baffin Bay at each location. The export of carbon from Jones Sound into Baffin Bay is roughly $1.23 \times 10^{14} \text{ g C yr}^{-1}$, while that from Lancaster Sound is roughly $3.25 \times 10^{14} \text{ g C yr}^{-1}$. The total carbon transport is then estimated at $4.48 \times 10^{14} \text{ g C yr}^{-1}$. Using the volume transport estimate of Ingram et al. (2002) for the Baffin Current ($1.7 \times 10^6 \text{ m}^{-3} \text{ s}^{-1}$), the outflows from Jones and Lancaster Sounds then supply roughly 18% and 65% of this water respectively, making the Arctic Archipelago an important source of both water and carbon to Baffin Bay and subsequently to the North Atlantic. Estimates of biological DIC draw down have been made for the North Water region (Yager et al., 1995; Miller et al., 2002), and they are of the same order of magnitude as estimates made in the southwestern Archipelago (Jull-Pedersen et al., 2010; Shadwick et al., 2011). However, our data do not indicate the same subsurface DIC excess at the Jones and Lancaster Sound outflows as was observed in the southwestern Archipelago (see Fig. 5a and Section 5.1). It has been suggested that changes in water column DIC in the North Water are driven by both biological processes and by advection, or transport of water with different concentration of DIC into or out of the region (Miller et al., 2002). It is likely that some of the subsurface DIC at Jones and Lancaster Sounds is the result of

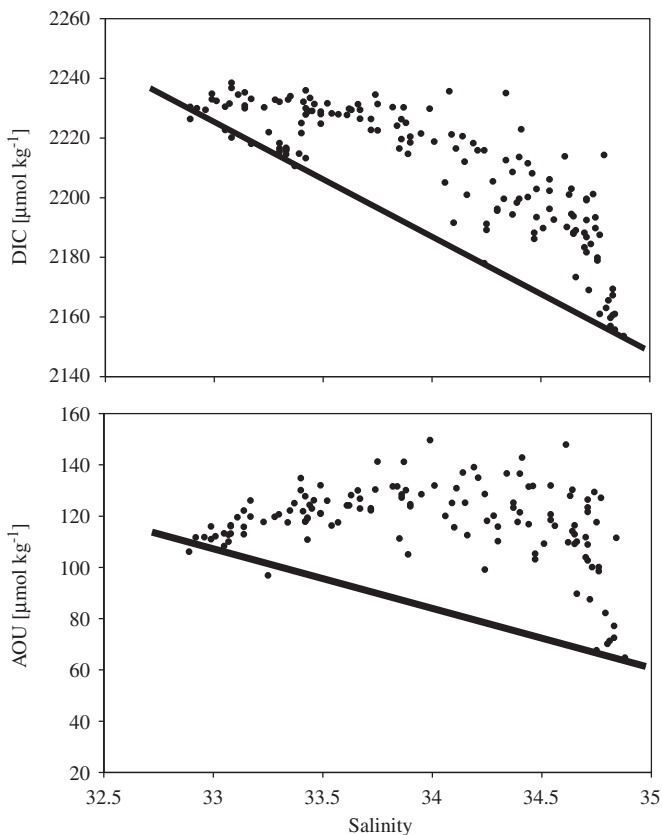


Fig. 7. Water masses of Pacific and Atlantic origin from the Beaufort sea are plotted in the top panel, while the corresponding AOU is plotted over the same salinity range in the bottom panel. Integrating $\Delta\text{DIC}_{\text{bio}}$, and AOU over the salinity range of Pacific ($S=33.1$) and Atlantic ($S=34.8$) waters yields a total carbon surplus, or respiration inventory, of $5.8 \pm 0.2 \text{ mol C m}^{-2}$, and a corresponding oxygen utilization of $7.7 \pm 0.5 \text{ mol O}_2 \text{ m}^{-2}$.

rem mineralization which occurred within the Archipelago with the resulting excess DIC transported through the Archipelago to Baffin Bay. Accurate quantification of this process, however, goes beyond the methods employed here.

The outflows from Jones and Lancaster Sound can be compared with water entering Baffin Bay via the WGC. This allows an estimate of carbon enrichment resulting from the outflows of the Archipelago, which contain Pacific-origin UHL waters with relatively higher DIC than the WGC waters. Salinity, DIC, and total alkalinity (TA) data from the Labrador Sea in 1998 (Jones, 1998) were corrected for the increased atmospheric, and subsequently oceanic, CO₂ concentration over the 10-year period since the data were collected. DIC and TA from the 1998 Labrador Sea data set were used to compute pCO₂ (Millero, 1994), which was then scaled up according to an increase of 1.7 ppm per year (Thomas et al., 2008). We have assumed that the surface ocean tracks this atmospheric increase of 1.7 ppm per year, and that additional factors, such as warming which would increase pCO₂, can be neglected. We have further assumed that TA remained constant over this 10 year period. TA and the augmented pCO₂ values were then used to compute the present day DIC concentrations. We assume that the most northeastern station of the Labrador Sea transect (Fig. 1) represents WGC water with a mean DIC concentration of 2125 μmol kg⁻¹. The outflow from the Archipelago via Jones and Lancaster Sounds, which includes the addition of Atlantic water from Nares Strait, has a DIC concentration of 2140 μmol kg⁻¹. The difference between these values allows us to estimate the carbon enrichment at roughly 15 μmol kg⁻¹, or 0.18 g C m⁻³.

5.3. Impact of increased sea-ice melt

Over the last few hundred years, the surface ocean pH has decreased by roughly 0.1 units (Caldeira and Wickett, 2003). A further pH decrease of 0.3 units has been predicted (Feely et al., 2004; Orr et al., 2005), and model results have indicated that high-latitude oceans will become undersaturated with respect to aragonite (i.e. $\Omega_{Ar} < 1$), and calcite before other regions (Orr et al., 2005; Fabry et al., 2009). The observed loss of sea-ice from the Arctic over the past decade has been faster than even the most pessimistic global model prediction (Moritz et al., 2002; Maslanik et al., 2007; Stroeve et al., 2007) and a sustained and wide-spread freshening of the Arctic has been reported (McPhee et al., 1998; Dickson, 1999; Lammers et al., 2001; Peterson et al., 2002, 2006). Furthermore, with a warming climate the Arctic hydrological cycle is expected to undergo additional change, and significant increases in precipitation have been projected (Peterson et al., 2006).

The addition of freshwater, particularly from sea-ice melt and precipitation which have very low concentrations of DIC and TA, to the surface of the Arctic Ocean dilutes the water with respect to its chemical constituents. It has recently been reported that increases in SIM in the Canada Basin have resulted in lower surface Ω_{Ar} (Chierici and Fransson, 2009; Yamamoto-Kawai et al., 2009). To assess the impact of changing the composition of water masses exiting the Archipelago, we varied the relative fraction of SIM in the upper 30 m of the Lancaster Sound outflow. By altering the amount of SIM, we consequently dilute the relative concentrations of surface DIC and TA flowing into Baffin Bay. To see the impact that such a change would have on acidification of the North Atlantic, the new pH and Ω_{Ar} are computed. The observed pH and Ω_{Ar} in upper 30 m of the water column in Lancaster Sound were 8.19 and 1.52, respectively. Undersaturation ($\Omega_{Ar} < 1$) of the surface waters was reached when the sea-ice melt fraction exceeded 30%; the corresponding pH was increased to a value

of 8.27 with this dilution of the surface waters. Dilution of the surface waters also decreases the pCO₂, and may potentially allow enhanced uptake of atmospheric CO₂ by the surface waters decreasing Ω_{Ar} and pH. On the other hand, ice-free surface waters in the Arctic will be considerably warmer than ice-covered waters, and the resulting thermodynamic increase in pCO₂ may outweigh the decrease due to dilution.

Pacific-origin UHL water has a higher DIC than both PML and ATL water (and a lower TA than Atlantic water) and consequently lower pH, and Ω_{Ar} . An increase in the UHL fraction in the outflow from Lancaster Sound would deliver waters with low pH and Ω_{Ar} to Baffin Bay, while a decrease in the fraction of UHL in this outflow would have the opposite effect. It can be seen from the distribution of pH in Fig. 5d that PML water has higher pH (and lower DIC and TA) than both the Pacific and Atlantic water. Photosynthesis in the surface waters decreases DIC and increases both pH and Ω_{Ar} , while respiration, or remineralization of organic matter, which takes place in the subsurface, at the level of the Pacific-origin core, increases DIC and decreases both pH and Ω_{Ar} . Increases in export production as a possible consequence of an extended growing season in the increasingly ice-free Arctic would increase the DIC and reduce the pH and Ω_{Ar} in the subsurface waters exiting the Archipelago, and potentially deliver more carbon-rich water to the North Atlantic. Export of high carbon Pacific water to the North Atlantic has implications for the uptake of anthropogenic carbon, and hence ocean acidification in this area. However, natural variability may also be important, and NAO and/or AO driven changes in the composition of waters leaving the Arctic may also influence carbon uptake and saturation states in the subpolar and temperate North Atlantic.

6. Conclusions

Inorganic carbon system data collected throughout the Canadian Arctic Archipelago allowed an assessment of the distribution and carbon characteristics of the water masses in this region. Meteoric water (MW) comprises roughly 3% of the surface waters in the western region of the Archipelago while sea-ice melt (SIM) water contributes roughly 4%. The fraction of MW decreases eastward contributing less than 1% to the surface waters in Jones and Lancaster Sounds. There is a corresponding increase in SIM from the western Archipelago to the eastern outflows to Baffin Bay. Low surface dissolved inorganic carbon (DIC) concentrations were observed in the upper water column throughout the Archipelago resulting from biological production and freshwater input with minimum DIC in the western region. The depth of penetration of Pacific-origin upper halocline water (UHL) increases eastward through the Archipelago. The export of carbon through the Archipelago to Baffin Bay at the outflows of Jones and Lancaster Sounds of 4.5×10^{14} g C m⁻² yr⁻¹ was estimated. In the subsurface waters of the western Archipelago there was a respiratory carbon surplus of 2.9–5.8 mol C m⁻² yr⁻¹, which was likely fueled by inputs of organic material from the surface layer and by benthic respiration.

Acknowledgments

This research is part of the Canadian IPY initiatives and the Circumpolar Flaw Lead System (CFL) Study, and was supported by the Natural Sciences and Engineering Research Council of Canada (NSERC), ArcticNet, and MetOcean Data Systems. The authors are grateful for the enthusiastic cooperation of the crew of the CCGS Amundsen and colleagues on board. We wish to thank Al Mucci for his insight and contribution to the field program, Nick Bates,

and two anonymous reviewers, for their helpful suggestions. This work contributes to IGBP/IHDP-LOICZ.

References

- Aagaard, K., Coachman, L.K., Carmack, E.C., 1981. On the halocline of the Arctic Ocean. *Deep-Sea Res.* 28, 529–545.
- Aagaard, K., Carmack, E.C., 1994. The Arctic Ocean and climate: a perspective. In: *The Polar Oceans and Their Role in Shaping the Global Environment*. AGU, Washington, DC.
- Anderson, L.G., Björk, G., Holby, O., Jones, E.P., Kattner, G., Koltermann, K.P., Liljeblad, B., Linderger, R., Rudels, B., Swift, J., 1994. Water masses and circulation in the Eurasian basin: results from the Oden 91 expedition. *J. Geophys. Res.* 99, 3273–3283.
- Anderson, L.G., Olsson, K., Chierici, M., 1998a. A carbon budget for the Arctic Ocean. *Global Biogeochem. Cycles* 12, 455–465.
- Anderson, L.G., Olsson, K., Jones, E.P., Chierici, M., Fransson, A., 1998b. Anthropogenic carbon dioxide in the Arctic Ocean: inventory and sinks. *J. Geophys. Res.* 103, 27,707–27,716.
- Anderson, L.G., Jutterström, S., Kaitin, S., Jones, E.P., Björk, G., 2004. Variability in river runoff distribution in the Eurasian Basin of the Arctic Ocean. *J. Geophys. Res.* 109, C01016.
- Arrigo, K.R., van Dijken, G.L., 2004. Annual cycles of sea ice and phytoplankton in Cape Bathurst polynya, southeastern Beaufort Sea, Canadian Arctic. *Geophys. Res. Lett.* 31, L08304.
- Arrigo, K.R., van Dijken, G., Pabi, S., 2008. Impact of a shrinking Arctic ice cover on marine primary production. *Geophys. Res. Lett.* 35, L19603.
- Bates, N.R., Best, M.H.P., Hansell, D.A., 2005. Spatio-temporal distribution of dissolved inorganic carbon and net community production in the Chukchi and Beaufort Seas. *Deep-Sea Res.* II 52, 3303–3323.
- Bates, N.R., Mathis, J.T., 2009. The Arctic Ocean marine carbon cycle: evaluation of air–sea CO₂ exchanges, ocean acidification impacts and potential feedbacks. *Biogeosciences* 6, 2433–2459.
- Bates, N.R., Mathis, J.T., Cooper, L., 2009. Ocean acidification and biologically induced seasonality of carbonate mineral saturation states in the western Arctic Ocean. *J. Geophys. Res.* 114, C11007.
- Caldeira, K., Wickett, M.E., 2003. Anthropogenic carbon and ocean pH. *Nature* 425, 365.
- Carmack, E., Chapman, D.C., 2003. Wind-driven shelf/basin exchange on an Arctic shelf: the joint roles of ice cover extent and shelf-break bathymetry. *Geophys. Res. Lett.* 30, 1778.
- Carmack, E.C., Macdonald, R.W., 2002. Oceanography of the Canadian shelf of the Beaufort sea: a setting for marine life. *Arctic* 55, 29–45.
- Carmack, E.C., Macdonald, R.W., Jasper, S., 2004. Phytoplankton productivity on the Canadian shelf of the Beaufort Sea. *Mar. Ecol. Prog. Ser.* 277, 37–50.
- Carmack, E., Wassmann, P., 2006. Food webs and physical–biological coupling on pan-Arctic shelves: unifying concepts and comprehensive perspectives. *Prog. Oceanogr.* 71, 446–477.
- Chierici, M., Fransson, A., 2009. Calcium carbonate saturation in the surface water of the Arctic Ocean: undersaturation in freshwater influenced shelves. *Biogeosciences* 6, 2421–2432.
- Coachman, L.K., Aagaard, K., 1974. Physical oceanography of Arctic and subarctic seas. In: Herman, T. (Ed.), *Marine Geology and Oceanography of the Arctic Seas*. Springer-Verlag, New York.
- Coachman, L.K., Aagaard, K., 1988. Transport through Bering Strait: Annual and interannual variability. *J. Geophys. Res.* 93, 15,535–15,539.
- Cooper, L.W., McClelland, J.W., Holmes, R.M., Raymond, P.A., Gibson, J.J., Peterson, B.J., 2008. Flow-weighted values of runoff tracers ($\delta^{18}\text{O}$, DOC, Ba, alkalinity) from the six largest Arctic rivers. *Geophys. Res. Lett.* 35, L118606. doi:10.1029/2008GL034007.
- Cota, G.F., Pomeroy, L.R., Harrison, W.G., Jones, E.P., Peters Jr., W.M.S.F., Weingartner, T.R., 1996. Nutrients, primary production and microbial heterotrophy in the southeastern Chukchi Sea: Arctic summer nutrient depletion and heterotrophy. *Mar. Ecol. Prog. Ser.* 135, 247–258.
- Cuny, J., Rhines, P.B., Kwok, R., 2005. Davis Strait volume, freshwater and heat fluxes. *Deep-Sea Res.* I 52, 519–542.
- Dickson, A.G., Millero, F.J., 1987. A comparison of the equilibrium constants for the dissociation of carbonic acid in seawater media. *Deep-Sea Res.* 34, 1733–1743.
- Dickson, B., 1999. All change in the Arctic. *Nature* 397, 389–391.
- Dittmar, T., Kattner, G., 2003. The biogeochemistry of the river and shelf ecosystem of the Arctic Ocean: a review. *Mar. Chem.* 83, 103–120.
- Ekwurzel, B., Schollosser, P., Mortlock, R.A., Fairbanks, R.G., Swift, J.H., 2001. River runoff, sea ice melt-water, and Pacific water distribution and mean residence times in the Arctic Ocean. *J. Geophys. Res.* 106, 9075–9092.
- Fabry, V.J., McClintock, J.B., Mathis, J.T., Grebeiner, J.M., 2009. Ocean acidification at high latitudes: the bellwether. *Oceanography* 22, 160–171.
- Falkner, K.K., Steele, M., Woodgate, R.A., Swift, J.H., Aagaard, K., Morison, J., 2005. Dissolved oxygen extreme in the Arctic Ocean halocline from the North Pole to the Lincoln Sea. *Deep-Sea Res.* I 52, 1138–1154.
- Feely, R.A., Sabine, C.L., Lee, K., Berelson, W., Kleypas, J., Fabry, V.J., Millero, F.J., 2004. Impact of anthropogenic CO₂ on the CaCO₃ system in the ocean. *Science* 305, 362–366.
- Forest, A., Sempel, M., Makabe, R., Sasaki, H., Barber, D.G., Gratton, Y., Wassmann, P., Fortier, L., 2008. The annual cycle of particulate organic carbon export in Franklin Bay (Canadian Arctic): environmental control and food web implications. *J. Geophys. Res.* 113, C03505.
- Fransson, A., Chierici, M., Anderson, L.G., Bussmann, I., Kattner, G., Jones, E.P., Swift, J.H., 2001. The importance of shelf processes for the modification of chemical constituents in the waters of the Eurasian Arctic Ocean: implication for carbon fluxes. *Cont. Shelf Res.* 21, 225–242.
- Friis, K., Körtzinger, A., Wallace, D.W.R., 2003. The salinity normalization of marine inorganic carbon chemistry data. *Geophys. Res. Lett.* 30, 1085.
- Greene, C.H., Pershing, A.J., 2007. Climate drives sea change. *Science* 315, 1084–1085.
- Hansell, D.A., Kadko, D., Bates, N.R., 2004. Degradation of terrigenous dissolved organic carbon in the western Arctic Ocean. *Science* 304, 858–861.
- Ingram, R.G., Båcle, J., Barber, D.G., Gratton, Y., Melling, H., 2002. An overview of physical processes in the North Water. *Deep-Sea Res.* II 49, 4893–4906.
- Johnson, K.M., Wills, K.D., Butler, D.B., Johnson, W.K., Wong, C.S., 1993. Coulometric total carbon dioxide analysis for marine studies: maximizing the performance of an automated gas extraction system and coulometric detector. *Mar. Chem.* 44, 167–188.
- Jones, P., 1998. Total CO₂ and total alkalinity data obtained during the R/V Hudson mission in the North Atlantic Ocean during WOCE section AR01W (AR07W) (22 June–9 July, 1998). Technical Report, Carbon Dioxide Information Analysis Center, Oak Ridge National Laboratory, Oak Ridge, Tennessee.
- Jones, E.P., Anderson, L.G., Swift, J.H., 1998. Distribution of Atlantic and Pacific waters in the upper Arctic Ocean: implications for circulation. *Geophys. Res. Lett.* 25, 765–768.
- Jones, E.P., Swift, J.H., Anderson, L.G., Lipizer, M., Civitarese, G., Falkner, K.K., Kattner, G., McLaughlin, F., 2003. Tracing Pacific water in the North Atlantic Ocean. *J. Geophys. Res.* 108, 3116.
- Jull-Pedersen, T., Michel, C., Gosselin, M., 2010. Sinking export of particulate organic material from the euphotic zone in the eastern Beaufort Sea. *Mar. Ecol. Prog. Ser.* 410, 55–70.
- Kaitin, S., Anderson, L.G., 2005. Uptake of atmospheric carbon dioxide in Arctic Seas: evaluation of the relative importance of processes that influence pCO₂ in water transported over the Bering–Chukchi Sea shelf. *Mar. Chem.* 94, 67–79.
- Khatiwala, S.P., Fairbanks, R.G., Houghton, R.W., 1999. Freshwater sources to the coastal ocean off northeastern North America: evidence from H₂¹⁸O/H₂¹⁶O. *J. Geophys. Res.* 104, 18,241–18,255.
- Lammers, R.B., Shiklomanov, A.I., Vorosmarty, C.J., Fekete, B.M., Peterson, B.J., 2001. Assessment of contemporary Arctic river runoff based on observational discharge records. *J. Geophys. Res.* 109, C01016.
- Lanos, R., 2009. Circulation régionale, masses d'eau, cycles d'évolution et transports entre la Mer de Beaufort et le Golfe d'Amundsen. Ph.D. Thesis, Université du Québec.
- Lewis, E., Wallace, D.W.R., 1998. Program developed for CO₂ systems calculations. ORNL/CDIAC 105, Carbon Dioxide Information Analysis Center, Oak Ridge National Laboratory US Department of Energy, Oak Ridge, Tennessee.
- Lobb, J., Weaver, A.J., Carmack, E.C., Ingram, R.G., 2003. Structure and mixing across an Arctic/Atlantic front in northern Baffin Bay. *Geophys. Res. Lett.* 30, 1833.
- Macdonald, R.W., Wong, C.S., Erickson, P.E., 1987. The distribution of nutrients in the southeastern Beaufort Sea: implications for water circulation and primary production. *J. Geophys. Res.* 92, 2939–2952.
- Macdonald, R.W., Carmack, E.C., McLaughlin, F.A., Falkner, K.K., Swift, J.T., 1999. Connections among ice, runoff and atmospheric forcing in the Beaufort Gyre. *Geophys. Res. Lett.* 26, 2223–2226.
- Macdonald, R.W., McLaughlin, F.A., Carmack, E.C., 2002. Fresh water and its sources during the SHEBA drift in the Canada Basin of the Arctic Ocean. *Deep-Sea Res.* I 49, 1769–1785.
- Macdonald, R.W., Anderson, L.C., Christensen, J.P., Miller, L.A., Semiletov, I.P., Stein, R., 2009. The Arctic ocean. In: Liu, K.K., Atkinson, L., Quinones, R., Talue-McManus, L. (Eds.), *Carbon and Nutrient Fluxes in Continental Margins: A Global Synthesis, Global Change—The IGBP Series*. Springer, New York, USA, pp. 293–301.
- Maslanik, J.A., Fowler, C., Stroeve, J., Drobot, S., Zwally, J., Yi, D., Emery, W., 2007. A younger, thinner Arctic ice cover: increased potential for rapid, extensive sea-ice loss. *Geophys. Res. Lett.* 34, L24501.
- Mathis, J.T., Hansell, D.A., Bates, N.R., 2005. Strong hydrographic controls on spatial and seasonal variability of dissolved organic carbon in the Chukchi Sea. *Deep-Sea Res.* II 52, 3245–3258.
- Mathis, J.T., Hansell, D.A., Kadko, D., Bates, N.R., Cooper, L.W., 2007. Determining net dissolved organic carbon production in the hydrographically complex western Arctic Ocean. *Limnol. Oceanogr.* 52, 1789–1799.
- Mathis, J.T., Bates, N.R., Hansell, D.A., Babila, T., 2009. Net community production in the northeastern Chukchi Sea. *Deep-Sea Res.* II 56, 1213–1222.
- McLaughlin, F.A., Carmack, E.C., Macdonald, R.W., Melling, H., Swift, J.H., Wheeler, P.A., Sherr, B.F., Sherr, E.B., 2004. The joint roles of Pacific and Atlantic-origin waters in the Canada Basin, 1997–1998. *Deep-Sea Res.* I 51, 107–128.
- McLaughlin, F.A., Carmack, E.C., Macdonald, R.W., Biship, J.K.B., 1996. Physical and geochemical properties across the Atlantic/Pacific water mass front in the southern Canadian Basin. *J. Geophys. Res.* 101, 1183–1197.
- McPhee, M.G., Stanton, T.P., Morison, J.H., Martinson, D.G., 1998. Freshening of the upper ocean in the Arctic: is perennial sea ice disappearing? *Geophys. Res. Lett.* 25, 1729–1732.
- Mehrbach, C., Culbertson, C.H., Hawley, J.E., Pytkowicz, R.M., 1973. Measurement of the apparent dissociation constants of carbonic acid in seawater at atmospheric pressure. *Limnol. Oceanogr.* 18, 897–907.

- Melling, H., Gratton, Y., Ingram, G., 2001. Ocean circulation within the North Water polynya of Baffin Bay. *Atmosphere-Ocean* 39, 301–325.
- Miller, L.A., Yager, P.L., Erickson, K.A., Amiel, D., Bâcle, J., Cochran, J.K., Garneau, M.-E., Gosselin, M., Hirschberg, D.J., Klein, B., LeBlanc, B., Miller, W.L., 2002. Carbon distributions and fluxes in the North Water, 1998 and 1999. *Deep-Sea Res. II* 49, 5151–5170.
- Millero, F.J., 1994. Thermodynamics of the carbon dioxide system in the oceans. *Geochem. Cosmochim. Acta* 59, 661–677.
- Millero, F.J., 2006. *Chemical Oceanography*. Taylor & Francis.
- Morison, J., Steele, M., Andersen, R., 1998. Hydrography of the upper Arctic Ocean measured from the nuclear submarine U.S.S. Pargo. *Deep-Sea Res.* 45, 15–38.
- Moritz, R.E., Bitz, C.M., Steig, E.J., 2002. Dynamics of recent climate change in the Arctic. *Science* 297, 1497–1502.
- Mucci, A., Lansard, B., Miller, L.A., Papakyriakou, T.N., 2010. CO₂ fluxes across the air–sea interface in the southeastern Beaufort Sea: the ice-free period. *J. Geophys. Res.* 297, 1497–1502.
- Münchow, A., Faulkner, K.K., Melling, H., 2007. Spatial continuity of measured seawater and tracer fluxes through Nares Strait, a dynamically wide channel bordering the Canadian Archipelago. *J. Mar. Res.* 65, 759–788.
- Orr, J.C., Fabry, V.J., Aumont, O., Bopp, L., Doney, S.C., Feely, R.A., Gnanadesikan, A., Gruber, N., Ishida, A., Joos, F., Key, R.M., Lindsay, K., Maier-Reimer, E., Matear, R., Monfray, P., Mouchet, A., Najjar, R.G., Plattner, G.-K., Rodgers, K.B., Sabine, C.L., Sarmiento, J.L., Schlitzer, R., Slater, R.D., Totterdell, I.J., Weirig, M.-F., Yamanaka, Y., Yool, A., 2005. Anthropogenic ocean acidification over the twenty-first century and its impact on calcifying organisms. *Nature* 437, 681–686.
- Peterson, B., Holmes, R.M., McClelland, J., Vorosmarty, C.J., Lammers, R.B., Shiklomanov, A.I., Shiklomanov, I.A., Rahmstorf, S., 2002. Increasing river discharge to the Arctic Ocean. *Science* 298, 2171–2173.
- Peterson, B., McClelland, J., Curry, R., Holmes, R.M., Walsh, J.E., Aagaard, K., 2006. Trajectory shifts in the Arctic and subarctic freshwater cycle. *Science* 313, 1061–1066.
- Prinsenberg, S., Hamilton, J., 2005. Monitoring the volume, freshwater and heat fluxes passing through Lancaster Sound in the Canadian Arctic Archipelago. *Atmosphere-Ocean* 43, 1–22.
- Rahmstorf, S., 2002. Ocean circulation and climate during the past 120,000 years. *Nature* 419, 207–214.
- Renaud, P.E., Riedel, A., Michel, C., Morata, N., Gosselin, M., Juul-Pedersen, T., Chiuchiolo, A., 2007. Seasonal variation in benthic community oxygen demand: a response to an ice algal bloom in the Beaufort Sea, Canadian Arctic? *J. Mar. Syst.* 67, 1–12.
- Revelle, R., Suess, H.E., 1957. Carbon dioxide exchange between atmosphere and ocean and the question of an increase of atmospheric CO₂ during the past decades. *Tellus* 9, 18.
- Robbins, P.E., 2001. Oceanic carbon transport carried by freshwater divergence: are salinity normalizations useful? *J. Geophys. Res.* 106, 30,939–30,946.
- Rudels, B., 1986. The outflow of polar water through the Arctic Archipelago and the oceanographic conditions in Baffin Bay. *Polar Res.* 4, 161–180.
- Rudels, B., Jones, E.P., Anderson, L.G., Kattner, G., 1994. On the origin and circulation of the Atlantic layer and intermediate depth waters in the Arctic Ocean. In: *The Polar Oceans and Their Role in Shaping the Global Environment*. AGU, Washington, DC.
- Rudels, B., Anderson, L.G., Jones, E.P., 1996. Formation and evolution of the surface mixed layer and halocline of the Arctic Ocean. *J. Geophys. Res.* 101, 8807–8821.
- Sabine, C.L., et al., 2004. The oceanic sink for anthropogenic CO₂. *Science* 305, 367–371.
- Shadwick, E.H., Thomas, H., Chierici, M., Else, B., Fransson, M., Michel, C., Miller, L.A., Mucci, A., Niemi, A., Papakyriakou, T.N., Tremblay, J.-É., 2011. Seasonal variability of the inorganic carbon system in the Amundsen Gulf region of the southeastern Beaufort Sea. *Limnol. Oceanogr.* 56 (1), 303–322. doi:10.4319/lo.2011.56.1.0303.
- Semiletov, I., Pipko, I., Repina, I., Shakhova, N.E., 2007. Carbonate chemistry dynamics and carbon dioxide fluxes across the atmosphere–ice–water interfaces in the Arctic Ocean: Pacific sector of the Arctic. *J. Mar. Syst.* 66, 204–226.
- Serreze, M.C., Barrett, A.P., Slater, A.G., Woodgate, R.A., Aagaard, K., Lammers, R.B., Steele, M., Moritz, R., Meredith, M., Lee, C.M., 2006. The large-scale freshwater cycle of the Arctic. *J. Geophys. Res.* 111, C11010.
- Smith, W.O., Gordon, L.L., 1997. Hyperproductivity of the Ross Sea (Antarctica) polynya during austral spring. *Geophys. Res. Lett.* 24, 233–236.
- Steele, M., Boyd, T., 1998. Retreat of the cold halocline layer in the Arctic Ocean. *J. Geophys. Res.* 103, 10,419–10,435.
- Stroeve, J., Holland, M.M., Meier, W., Scambos, T., Serreze, M., 2007. Arctic sea ice decline: faster than forecast. *Geophys. Res. Lett.* 34, L09501.
- Takahashi, T., Olafsson, J., Goddard, J.G., Chipman, D.W., Sutherland, S.G., 1993. Seasonal variation of CO₂ and nutrients in the high-latitude surface oceans: a comparative study. *Global Biogeochem. Cycles* 7, 843–878.
- Thomas, H., Prowe, A.E.F., van Heuven, S., Bozec, Y., de Baar, H.J.W., Schiettecatte, L.-S., Suykens, K., Koné, M., Borges, A.V., Lima, I.D., Doney, S.C., 2007. Rapid decline of the CO₂ buffering capacity in the North Sea and implications for the North Atlantic Ocean. *Global Biogeochem. Cycles* 21. doi:10.1029/2006GB002825.
- Thomas, H., Prowe, F., Lima, I.D., Doney, S.C., Wanninkhof, R., Greatbatch, R.J., Schuster, U., Corbière, A., 2008. Changes in the North Atlantic oscillation influence CO₂ uptake in the North Atlantic over the past 2 decades. *Global Biogeochem. Cycles* 22 doi:10.1029/2007GB003167.
- Thompson, D.W., Wallace, J.M., 2001. Regional climate impacts of the Northern Hemisphere annular mode. *Science* 293, 85–89.
- Tremblay, J.-É., Simpson, K., Martin, J., Gratton, L.M.Y., Barber, D., Price, N.M., 2008. Vertical stability and the annual dynamics of nutrients and chlorophyll fluorescence in the coastal, southeast Beaufort Sea. *J. Geophys. Res.* 113, C07S90.
- Vallières, C., Retamal, L., Ramlal, P., Osburn, C.L., Vincent, W.F., 2008. Bacterial production and microbial food web structure in a large arctic river and the coastal Arctic Ocean. *J. Mar. Syst.* 74, 756–773.
- Yager, P.L., Wallace, D.W.R., Johnson, K.M., Smith Jr., W.O., Minnett, P.J., Deming, J.W., 1995. The Northeast Water Polynya as an atmospheric CO₂ sink: A seasonal rectification hypothesis. *J. Geophys. Res.* 100, 4389–4398.
- Yamamoto-Kawai, M., Tanaka, N., 2005. Freshwater and brine behaviors in the Arctic Ocean deduced from historical data of δ¹⁸O and alkalinity (1992–2002 a.d.). *J. Geophys. Res.* 110, C10003.
- Yamamoto-Kawai, M., McLaughlin, F.A., Carmack, E.C., Nishino, S., Shimada, K., 2009. Aragonite undersaturation in the Arctic Ocean: effects of ocean acidification and sea ice melt. *Science* 326, 1098–1100.
- Zeebe, R.E., Wolf-Gladrow, D., 2001. *CO₂ in Seawater: Equilibrium, Kinetics, Isotopes*. Elsevier, Amsterdam.